Applied Surface Science 334 (2015) 210–215

Contents lists available at ScienceDirect

Applied Surface Science

journal homepage: www.elsevier.com/locate/apsusc

Growth evolution of self-textured ZnO films deposited by magnetron sputtering at low temperatures

J.R.R. Bortoleto[a,*], M. Chaves[a], A.M. Rosa[b], E.P. da Silva[a], S.F. Durrant[a], L.D. Trino[c], P.N. Lisboa-Filho[c]

[a] Technological Plasmas Laboratory, São Paulo State University-UNESP, Av. Três de Março, 511, Sorocaba, SP, Brazil
[b] School of Electrical and Computer Engineering, University of Campinas-UNICAMP, Av. Albert Einstein, Campinas, SP, Brazil
[c] Group of Advanced Materials, São Paulo State University-UNESP, Av. Eng. Luiz Edmundo Carrijo Coube, 14-01, Bauru, SP, Brazil

ARTICLE INFO

Article history:
Received 13 June 2014
Received in revised form 1 October 2014
Accepted 1 October 2014
Available online 20 October 2014

Keywords:
Surface texturing
ZnO thin films
Magnetron sputtering
Low temperature
Growth evolution

ABSTRACT

In this work, the evolution of the surface morphology of ZnO thin films deposited by reactive RF magnetron sputtering has been investigated using atomic force microscopy (AFM) and X-ray diffraction (XRD). All AFM images of the films were analyzed using scaling concepts. To study the growth evolution, different ZnO films with thicknesses of up to 1270 nm were deposited at temperatures of 100 and 250 °C. For the films grown at 100 °C, AFM data show that the lateral length ξ evolves continuously while the temporal evolution of the root mean square roughness σ presents two distinct regimes. Early during the depositions, the morphology of the ZnO films is mainly characterized by granular structures. Beyond thickness of about 600 nm, pyramid-like structures with {214} crystallographic facets start to develop. For the films grown at 250 °C, however, only one growth regime was observed and for the thicker films, the surface morphology consisted of polygonal structures. For the films grown at 100 °C, the growth exponents, β, and the exponent defining the evolution of the characteristic wavelength of the surface, p, were $\beta_1 = 0.70 \pm 0.02$ and $\beta_2 = 0.26 \pm 0.2$; and $p = 0.2 \pm 0.04$. For the films grown at 250 °C, the exponent values were $\beta = 0.78 \pm 0.02$ and $p = 0.32 \pm 0.05$. These values of the exponents indicate the occurrence of surface mechanisms, such as shadowing and surface diffusion, as well as facet stabilization at 100 °C. For the films grown at 250 °C, however, structural misorientation during growth also plays an important role.

1. Introduction

Currently there is great demand for transparent conductive oxides (TCOs), mainly for applications in solar cells and optoelectronic devices, such as organic light-emitting diodes (OLEDs) and flexible displays [1–3]. One of the most commonly used materials for TCOs is doped indium tin oxide (ITO), but ITO is relatively expensive, owing mainly to the scarcity of the element indium and the recent increase in its use in industrial applications [1]. Therefore, there is demand for a substitute for ITO. Zinc oxide (ZnO) has received attention owing to its many advantages, particularly high optical transmittance in the visible region, a wide band gap of 3.37 eV, low toxicity, low production cost, and the abundance of the chemical element zinc in nature [1–5]. More recently, ZnO has been used as an n-type layer in heterojunction Cu_2O thin film solar cells [4].

Several techniques have been employed for the production of ZnO thin films, including chemical vapor deposition (CVD) [6], sol–gel method [7], pulsed laser deposition [8], and magnetron sputtering [9–11]. Among these, magnetron sputtering has great potential due to the good adhesion of the films to the substrate, the possibility of deposition over large areas, and the high deposition rate [2]. More specifically, magnetron sputtering allows the synthesis of thin films at low temperatures, which makes it ideal for the deposition of thin films on polymeric substrates [2,5].

The study of the evolution of the film morphology is interesting because many applications depend strongly on the surface roughness [12,13]. For example, a textured surface may increase light scattering and thus improve the performance of a solar cell [3,4,13]. In addition, the texture is often related to a preferred orientation (PO) of the polycrystalline grains [12]. Therefore, controlling the PO could allow the selection of the desired properties [12]. In sputtering, however, experimental parameters such as the film thickness [9], the plasma power [14], and the substrate temperature [15–18],

* Corresponding author. Tel.: +55 1532383406.
E-mail addresses: jrborto@sorocaba.unesp.br, bortoleto.j2r@gmail.com (J.R.R. Bortoleto).

http://dx.doi.org/10.1016/j.apsusc.2014.10.015
0169-4332/

change the final texture. Consequently, it has been a challenge to find the dominant phenomena responsible for the PO as well as the surface texture [12]. Furthermore, stochastic processes such as shadowing, diffusion bias, and surface diffusion between planes or between grains can act during the nucleation and growth stages, affecting the final texture of polycrystalline films [19,20].

Based on these considerations, in this work, the evolution of the structural and surface morphology of ZnO thin films deposited by reactive RF magnetron sputtering has been investigated at two growth temperatures: 100 and 250 °C. The influence of the morphological evolution on the optical properties is also discussed.

2. Experimental details

ZnO films were deposited onto glass substrates using reactive RF magnetron sputtering. A metallic zinc target of 76.2 mm diameter and 99.99% purity was used as the zinc source. The target to substrate distance was 50 mm. Gas flows were controlled using needle valves and a mass flow controller (MKS 1179A). The plasma was activated by a 13.56 MHz RF source (with impedance matching, Tokyo Hy-Power Labs) at a power of 70 W. The partial pressure of oxygen and argon were set at a ratio of 1:10 and the total pressure was held at 1.4 Pa during the process. Before each deposition, the target was sputtered with argon for 10 min to remove the native oxide layer. The growth rates measured were (7.7 ± 0.2) and (6.7 ± 0.1) nm/min for series grown at 100 and 250 °C, respectively. During the deposition process, the temperature was controlled to within about ±5 °C.

The surface topography of the samples was investigated using atomic force microscopy (AFM, XE-100 Park Systems) operating in the non-contact mode. The scan size was $2 \times 2\ \mu m^2$ with 512×512 pixels. From the AFM measurements, the surface roughness was quantified using the root mean square (RMS) roughness, σ [19,21]. RMS roughness data were obtained directly from the AFM images using the 1.8.0 build16 data processing & analysis XEI software (Park Systems). Surface roughness is mathematically defined by Eq. (1).

$$\sigma = \sqrt{\frac{1}{N}\sum_{i=1}^{N}\left(h_i - \langle h \rangle\right)^2} \quad (1)$$

In this equation, N is the number of pixels, h_i the individual heights, and $\langle h \rangle$ the mean height. The lateral correlation length ξ was calculated from a Lorentz fitting of the power spectral density (PSD) curves in 2D provided by the AFM images using the same software [19,21]. This correlation length is statistically related to the lateral size evolution of the surface structures. Optical transmittance and reflectance spectra of the films were measured using an ultraviolet–visible-near infrared (UV–Vis-NIR) spectrometer from Perkin Elmer (model Lambda 750). Spectra were acquired over the wavelength range of 250–2500 nm. Transmittance measurements were used to estimate the film thickness, optical energy gap (E_g) and the average optical transmittance. The orientation and size of crystallites constituting the ZnO films were measured using an X-ray diffractometer (D/MAX-2100/PC, Rigaku), which employs the Cu Kα radiation (λ = 1.54056 Å) at grazing incidence (3°). Additionally, the microstructure was also characterized by scanning electron microscope (JEOL JSM-7500F).

3. Results and Discussion

Many studies report that increasing the substrate temperature changes the PO from the *a*-axis to the *c*-axis. Thus, according to Kajikawa's report [12] increasing the substrate temperature is considered to favor *c*-axis PO. We reported recently that in the substrate temperature range from 50 to 150 °C, the textured structure of our ZnO films grows with *c*-axis PO [18]. Heating the substrate in the temperature range from 200 to 250 °C, however, the misorientation of the crystallographic planes with the substrate surface is enhanced, indicating that a mixed *a*-axis and the *c*-axis textured surface can take place [18]. In addition, our AFM results also revealed a morphological transition at about 150 °C, resulting in a surface formed by grains with irregular shapes. These grains increased continuously in lateral size and height as the substrate temperature increased. Therefore, surface mechanisms such as shadowing and surface diffusion play an important role in the growth dynamics and change the preferred orientation. In the present investigation, to study the growth evolution of both pyramid-like and irregular grains, two series of ZnO films were grown at 100 and 250 °C, respectively.

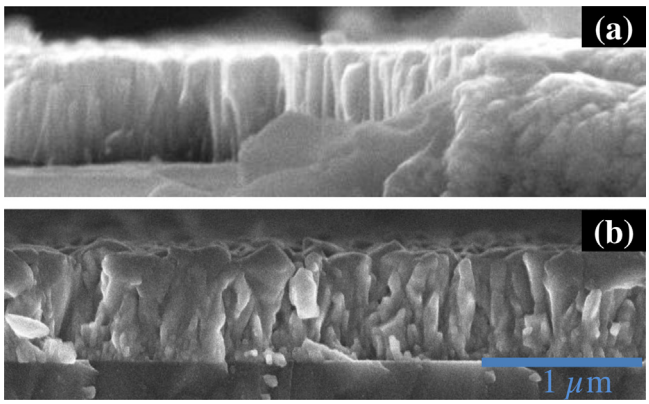

Fig. 1. Cross-sectional scanning electron micrographs of the surface texture of ZnO films deposited at (a) 100 °C (600 nm thick) and (b) 250 °C (595 nm).

3.1. Surface morphology

Fig. 1 shows cross-sectional scanning electron micrographs of the ZnO films with thicknesses of 600 and 595 nm deposited at 100 and 250 °C, respectively. In agreement with our previous work [18], distinct structures are clearly observed. For the film grown at 100 °C, columnar grains extend from the substrate to the top of the film can be observed. In contrast, films grown at 250 °C develop larger, irregular grains. As shown in Figs. 2 and 3, respectively, the surface morphology of the ZnO films grown at 100 and 250° C was also investigated using AFM images. All films exhibit a surface formed by granular structures at early stages, in which the lateral size ξ increases with increasing film thickness. As a consequence, the final texture depends on the film thickness as well as the substrate temperature.

Fig. 2 shows $2\ \mu m \times 2\ \mu m$ AFM images of the series grown at 100 °C. In Fig. 2(a)–(d), which corresponds to the ZnO films of thicknesses of 100, 140, 250 and 368 nm, respectively, the surface morphology reveals small regular grains with average ξ in the range of 50 to 65 nm. In Fig. 2(e), the film of thickness 600 nm still exhibits grains with regular shapes but with ξ of ≈110 nm. On the other hand, as seen in Fig. 2(f), for a film thickness of 1270 nm, there is the formation of a distinct surface structure. In this case, the surface morphology is formed by textured pyramid-like structures [19,22]. Shinagawa et al. [22] reported that this surface structure is suitable for light-trapping in Cu_2O solar cells. In particular, they observed six-folded pyramidal structures composed of (101) planes on top. As a consequence, the angle of the pyramidal structures at the surface is about 64°. Fig. 4 shows a surface profile taken of a $500 \times 500\ nm^2$ AFM image of the thicker ZnO film (1270 nm) grown at 100 °C. The formation

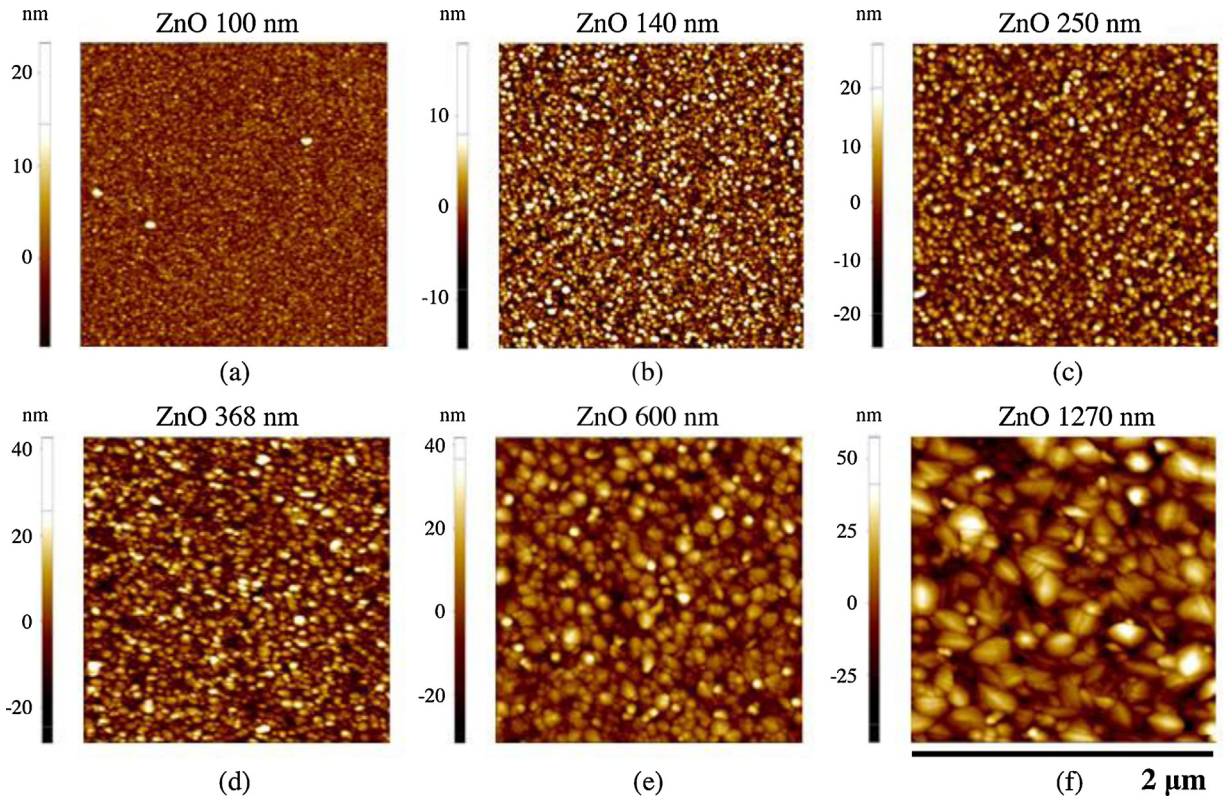

Fig. 2. 2 μm × 2 μm AFM images of the ZnO films deposited at 100 °C with different thicknesses: (a) 100; (b) 140; (c) 250; (d) 368; (e) 600; (f) 1270 nm.

of faceted grains is evident. Measurement of the grain angle revealed a value of ≈32°. Thus, the face with an angle of ≈32° exhibits planes compatible with {214} crystallographic planes of a hexagonal cell [23]. This angle tends to be retained since it is chemically more stable than a stepped surface. Therefore, lower angles indicate stepped surfaces in evolution. Greater angles were not observed, indicating that facet formation is energetically favorable [23].

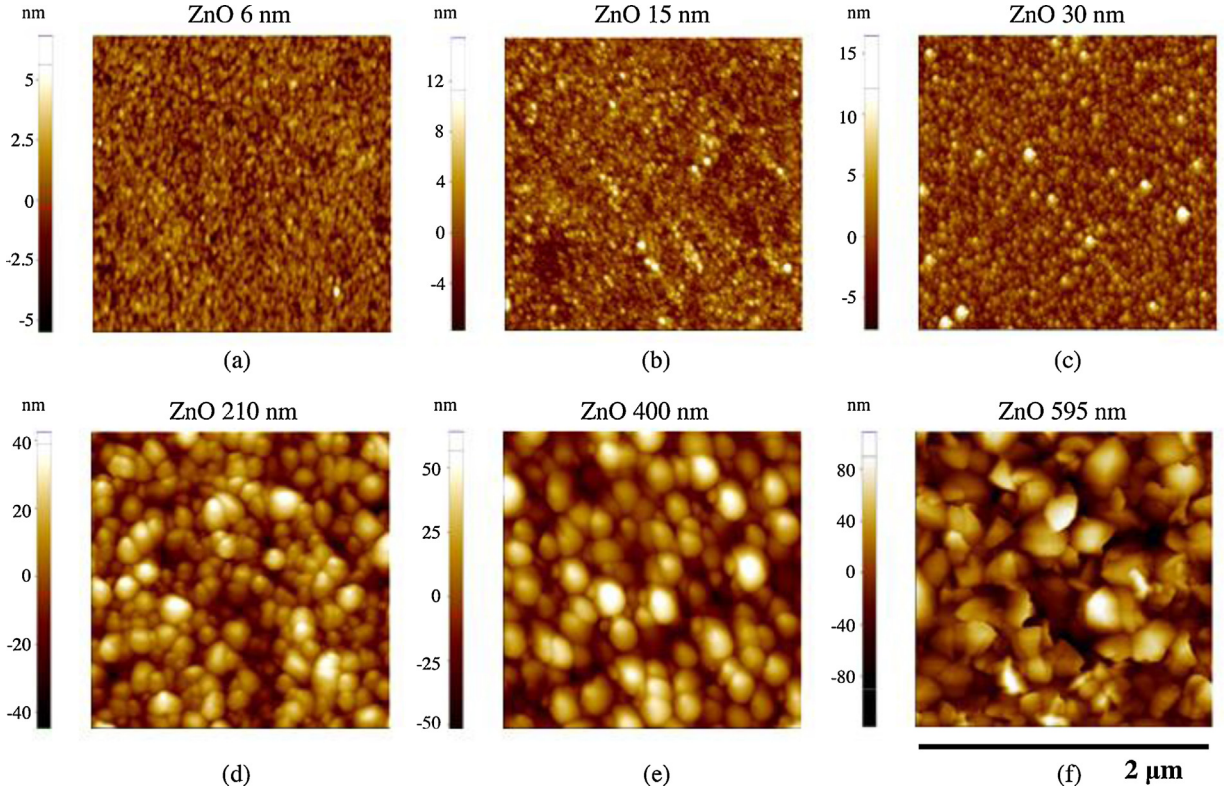

Fig. 3. 2 μm × 2 μm AFM images of the ZnO films deposited at 250 °C with different thicknesses: (a) 6; (b) 15; (c) 30; (d) 210; (e) 400; (f) 595 nm.

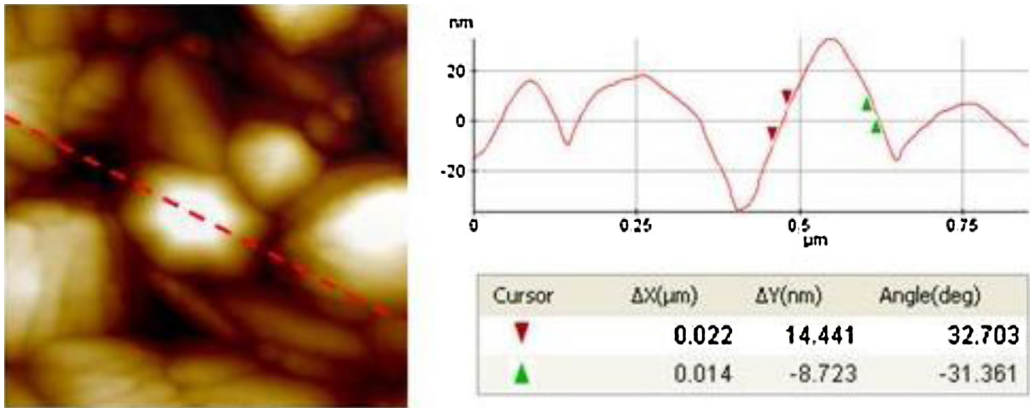

Fig. 4. Surface profile taken from a 500 nm × 500 nm AFM image of 1270 nm—thick ZnO film with $\xi = 179$ nm.

The typical small grains of the surface morphology of the films grown at 100 °C are also seen during the early growth stages for the films deposited at 250 °C. As deposition continues, however, the lateral size of the structures evolves until an irregular structure is formed (as seen in Fig. 3(f)). Indeed, for the thicker film (600 nm), the distinct surface feature is the formation of polygonal structures [24]. For these films, no {214} faceted pyramidal structures were observed.

Fig. 5 shows the evolution of the RMS surface roughness σ of the ZnO films grown at 100 and 250 °C. In addition, the roughness σ of ZnO films grown at <80 °C is included [21]. The roughness σ of the glass substrate was about 0.5 nm. From AFM data of the films deposited at 100 °C, σ evolves with increasing film thickness from ≈5 to ≈15 nm, indicating grain growth along the vertical direction.

For the films grown at 100 °C, the temporal evolution of the roughness σ presents two distinct regimes. The roughness exponents were found to be $\beta_1 = 0.70 \pm 0.02$ and $\beta_2 = 0.26 \pm 0.2$ for the consecutive regimes. Similar behavior is also described by Vasco et al. [19] for the growth of ZnO thin films on InP (100) substrates kept at 350 °C using pulsed laser deposition (PLD). In this case, Vasco et al. [19] found $\beta_1 = 1.0 \pm 0.1$ and $\beta_2 = 0.60 \pm 0.01$, respectively.

At lower temperatures (<80 °C) we observe that $\beta = 0.76 \pm 0.08$ and $p = 0.30 \pm 0.05$ but there is no saturation [21]. Mohanty et al. [20] found $\beta = 1.03 \pm 0.01$ for ZnO:Al thin film growth on glass substrates at room temperature by non-reactive magnetron sputtering, also indicating a single growth regime.

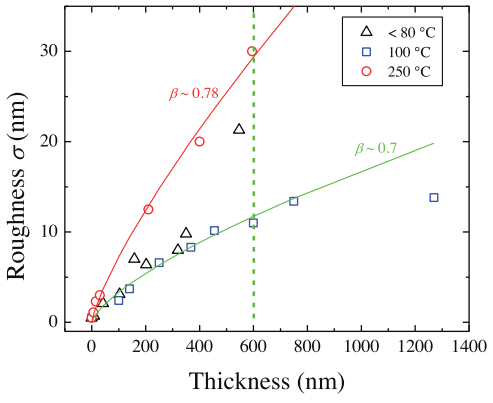

Fig. 5. The surface roughness σ as a function of the thickness as determined from 2 μm × 2 μm AFM images for different substrate temperatures. Open triangles, squares and circles are used to indicate the roughness of the ZnO films grown at <80, 100 and 250 °C, respectively. The surface roughness σ of the glass substrate is ≈0.5 nm. Continuous lines represent power law growth with exponent $\beta \approx 0.78$ and 0.70. The vertical dashed line indicates the transition observed at 100 °C.

For the ZnO films grown at 250 °C, σ evolves with the film thickness from ≈1 to ≈30 nm, indicating grain growth in the vertical direction. In this case, only one β value is found, $\beta = 0.7 \pm 0.02$, indicating a single growth regime. Thus, both the deposition processes of the ZnO films are initially characterized by unstable growth, since β is ≥0.5, resulting in the formation of textured surfaces [17,19].

From the experimental results obtained for the ZnO films it is possible to estimate the dominant growth mechanisms operating during deposition from the exponent β. Therefore, Vasco et al. [19] and Mohanty et al. [20] found $\beta = 1.0$, and they reported that the dominant mechanism is non-local shadowing, since this results in an unstable growth effect, thus increasing β. Although Vasco et al. [19] found $\beta_2 = 0.60$ and indicated that in this morphological region the Schwoebel barrier effect is the dominant mechanism, resulting in pyramidal structures with stepped surfaces, the occurrence of such mechanism is unlikely in polycrystalline systems with small grains [19]. For example, Fu and Shen [25] found $\beta = 0.56$ for Al films deposited on Si (100) substrates by magnetron sputtering, and concluded that non-local shadowing acting simultaneously with diffusion mechanisms result in a decrease in β.

Thus, one can recognize that the dynamic growth of ZnO films at 100 °C is initially driven by competition between shadowing and surface diffusion. Actually, $\beta_1 = 0.70$ implies that the shadowing determines the growth but surface diffusion is also present to a small degree. In the second regime, $\beta_2 = 0.26$, the surface morphology is steady in textured pyramid-like structures, indicating a shift in the dominant mechanism. Thus when {214} facetted texture becomes dominant the evolution of the surface roughness becomes more stable.

By heating the substrate to 250 °C, it is expected that surface diffusion acts strongly in the growth of the ZnO films and, as a consequence, a flatter surface should be obtained. But, as shown in Fig. 5, this behavior is not observed. Instead the formation of polygonal structures takes place, which indicates that another driving mechanism is dominant. Indeed, as reported by Kajikawa [12], for polycrystalline films surface diffusion can occur between grains or planes resulting in different PO and texture. In the case of surface diffusion that occurs between planes but is constrained by the grain contours, the film becomes non-equiaxial columnar with a surface texture and *c*-axis PO. If diffusion between grains is the dominant mechanism, the film becomes non-equiaxial columnar without surface texture and *a*-axis PO. If these two diffusion mechanisms are in competition, however, a non-equiaxial columnar rough film is produced such as that observed at 250 °C. Moreover,

no PO is observed because planes with higher surface energies as well as lower surface energies can coexist during growth. To further investigate this point, we present and discuss the XRD measurements in the next section.

3.2. Structural studies

Fig. 6(a) and (b) displays the X-ray diffraction patterns for ZnO films of different thicknesses deposited at 100 and 250 °C, respectively. It is possible to identify peaks corresponding to the characteristic planes of the hexagonal ZnO wurtzite structure, indicating that all films are polycrystalline (according to JCPDS 65-3411). For all of the films, the peak corresponding to the (002) plane is the most intense, indicating a preferential growth of the films along the *c*-axis, perpendicular to the substrate surface [12]. No peak was observed for the ZnO film thinner than 30 nm. A typical X-ray pattern can be seen in Fig. 6(b) for the 30 nm thick-ZnO film. This result indicates the formation of a ZnO amorphous layer during the early growth stages as reported by Chiang et al. [26]. Here, there is no preferential nucleation and the polycrystalline grains nucleate inside the amorphous layer.

From the X-ray diffraction spectra in Fig. 6(b), thicker films at 250 °C clearly exhibit reflections that correspond to peaks on planes (100) and (101), though the (002) peak remains dominant. These additional peaks indicate that the grains are not completely aligned along to *c*-axis [10], which implies that a polycrystalline film with more disordered crystallites is produced. From the kinetic point of view, this reinforces the interpretation that surface diffusion between planes and between grains are comparable and no PO takes place during growth.

In addition, the FWHM of the strongest (002) peak was used to estimate the crystallite size by employing Scherrer's formula [10]. The data for both series are plotted as a function of this thickness in Fig. 7(a). The crystallite size increases continuously and then saturates at 12 nm. On the other hand, the lateral length ξ of the ZnO films was found to grow continuously for both substrate temperatures of 100 and 250 °C. For the films deposited at 100 °C, the exponent $p = 0.2 \pm 0.04$ while, for that grown at 250 °C, this value is higher, $p = 0.32 \pm 0.05$. Although these values are lower than those reported by Vasco et al. [19], who found $p_1 = 0.33 \pm 0.05$ and $p_2 = 0.43 \pm 0.08$ for the consecutive growth regimes, these results indicate that the lateral size of surface structures is not directly related to the crystallite size since the first increases continuously rather than saturating.

Also according to the XRD patterns of the films, for both temperatures, there are shifts in the position of the (002) peak at greater thicknesses. Indeed, the position of the (002) peak is <34.42°, the value of bulk ZnO (JCPDS 65-3411), indicating that all films suffer compressive stress during the initial stage. The lattice constant *c*

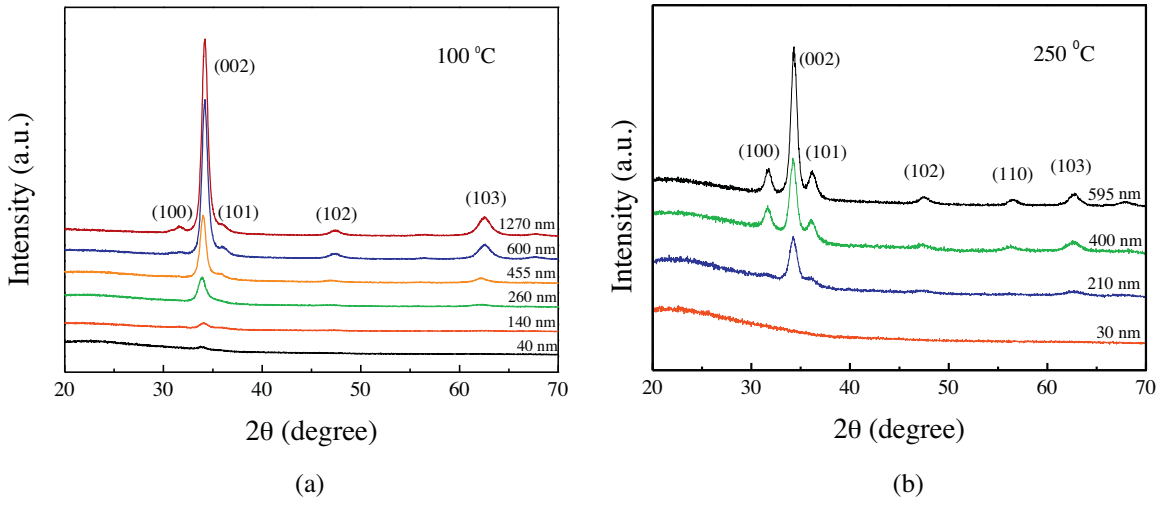

Fig. 6. XRD patterns of ZnO films grown at (a) 100 and (b) 250 °C with thicknesses as indicated.

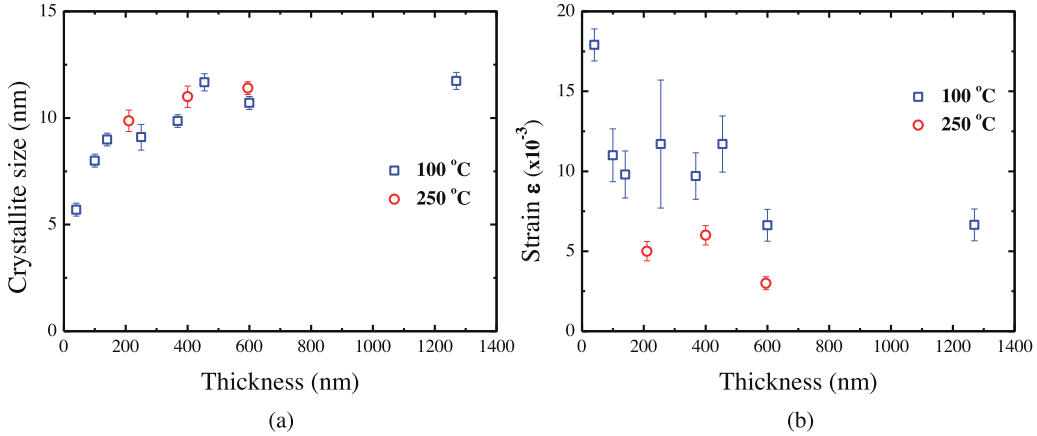

Fig. 7. (a) Crystallite size and (b) strain of the ZnO films as a function of the thickness. Opens squares and circles correspond to data obtained from films deposited at 100 and 250 °C, respectively.

was obtained from the position of the (002) peak for all films in both cases, and was used to estimate the strain ε in the films along the c-axis [10]. Fig. 7(b) displays the variation of the strain with increasing thickness. In both cases, the strain tends to decrease as thickness increases.

4. Conclusions

In conclusion, it has been observed that the surface morphology of ZnO films is initially characterized by small grains. As the deposition proceeds, increases in both lateral and vertical grain dimensions are observed. Thus, for the ZnO films grown at 100 °C, AFM data show that the correlation length evolves continuously while the temporal evolution of the roughness σ presents two distinct regimes. In the first regime, the morphology of ZnO films is dominated by granular structures. In the second regime, for longer deposition times, {214} faceted pyramid-like structures are produced, aligned along the (002) plane, and stabilizing the roughening process.

For ZnO films grown at 250 °C, similar behavior is observed, but with only one regime and, for thicker films, the surface features are formed by polygonal structures. In this case, the diffusion between planes and between grains is comparable, such that misorientation becomes important to the final texture. As a consequence, a non-equiaxial columnar rough film is produced.

Acknowledgments

The financial support of the Brazilian agencies FAPESP (Proc. 2008/53311-5 and 2011/21345-0) and CNPq (Proc. 555774/2010-4 and 301622/2012-4) is gratefully acknowledged.

References

[1] D.S. Ginley, Handbook of Transparent Conductors, 1st ed., Springer, New York, 2010.
[2] K. Elmer, Transparent Conducting Zinc Oxide and its Derivatives: Basics and Applications in Thin Film Solar Cells, 1st ed., Springer, New York, 2008.
[3] V. Avrutin, N. Izyumskaya, H. Morkoç, Semiconductor solar cells: recent progress in terrestrial, Superlattices Microstruct. 49 (2011) 337.
[4] T. Gershon, K.P. Musselman, A. Marin, R.H. Friend, J.L. MacManus-Driscoll, Thin-film ZnO/Cu_2O solar cells incorporating an organic buffer layer, Solar Energy Mater. Sol. Cells 96 (2012) 148.
[5] Y. Jouane, S. Colis, G. Schmerber, A. Dinia, P. Lévêque, T. Heiser, Y.A. Chapuis, Influence of flexible substrates on inverted organic solar cells using sputtered ZnO as cathode interfacial layer, Org. Electron. 14 (2013) 1861.
[6] Y.S. Choi, D.K. Hwang, B.J. Kwon, J.W. Kang, Y.H. Cho, S.J. Park, Effect of VI/II gas ratio on the epitaxial growth of ZnO films by metalorganic chemical vapor deposition, Jpn. J. Appl. Phys. 50 (2011) 105502.
[7] C.Y. Tsay, K.S. Fan, S.H. Chen, C.H. Tsai, Preparation and characterization of ZnO transparent semiconductor thin films by sol–gel method, J. Alloys Compd. 495 (2010) 126.
[8] E. Fazio, S. Patanè, S. Scibilia, A.M. Mezzasalma, G. Mondio, F. Neri, S. Trusso, Structural and optical properties of pulsed laser deposited ZnO thin films, Curr. Appl. Phys. 13 (2013) 710.
[9] F. Wang, M.Z. Wu, Y.Y. Wang, Y.M. Yu, X.M. Wu, L.J. Zhuge, Influence of thickness and annealing temperature on the electrical, optical and structural properties of AZO thin films, Vacuum 89 (2013) 127.
[10] S. Singh, R.S. Srinivasa, S.S. Major, Effect of substrate temperature on the structure and optical properties of ZnO thin films deposited by reactive RF magnetron sputtering, Thin Solid Films 515 (2007) 8718.
[11] M. Yuste, R. Escobar Galindo, I. Caretti, R. Torres, O. Sanchez, Influence of the oxygen partial pressure and post-deposition annealing on the structure and optical properties of ZnO films grown by dc magnetron sputtering at room temperature, J. Appl. Phys. 45 (2012) 025303.
[12] Y. Kajikawa, Texture development of non-epitaxial polycrystalline ZnO films, J. Cryst. Growth 289 (2006) 387.
[13] H. Zhu, Y. Mai, M. Wan, J. Gao, Y. Wang, T. He, Y. Feng, J. Yin, J. Du, J. Wan, R. Sun, Y. Huang, Study of back reflectors for thin film silicon solar cells, Thin Solid Films (2013) 284.
[14] P. Mondal, D. Das, Transparent and conducting intrinsic ZnO thin films prepared at high growth-rate with c-axis orientation and pyramidal surface texture, Appl. Surf. Sci. 286 (2013) 397.
[15] Z. Zhang, C. Bao, W. Yao, S. Ma, L. Zhang, S. Hou, Influence of deposition temperature on the crystallinity of Al-doped ZnO thin films at glass substrates prepared by RF magnetron sputtering method, Superlattices Microstruct. 49 (2011) 644.
[16] B. Singh, Z.A. Khan, I. Khan, S. Ghosh, Highly conducting zinc oxide thin films achieved without postgrowth annealing, Appl. Phys. Lett. 45 (2010) 241903.
[17] R. Wen, L. Wang, X. Wang, G.H. Yue, Y. Chen, D.L. Peng, Influence of substrate temperature on mechanical, optical and electrical properties of ZnO:Al films, J. Alloys Compd. 508 (2010) 370.
[18] A.M. Rosa, E.P. da Silva, M. Chaves, L.D. Trino, P.N. Lisboa-Filho, T.F. da Silva, S.F. Durrant, J.R.R. Bortoleto, Structural transition of ZnO thin films produced by RF magnetron sputtering at low temperatures, J. Mater. Sci.: Mater. Electron. (2013), ISSN: 0957-4522.
[19] E. Vasco, C. Zaldo, L. Vázquez, Growth evolution of ZnO films deposited by pulsed laser ablation, J. Phys.: Condens. Matter 13 (2001) L663.
[20] B.C. Mohanty, H.R. Choi, Y.S. Cho, Fluctuations in global surface scaling behavior in sputter-deposited ZnO thin films, Europhys. Lett. 93 (2011) 26003.
[21] A.M. Rosa, E.P. da Silva, E. Amorim, M. Chaves, A.C. Catto, P.N. Lisboa-Filho, J.R.R. Bortoleto, Growth evolution of ZnO thin films deposited by RF magnetron sputtering, J. Phys.: Conf. Ser. 370 (2012) 012020, http://dx.doi.org/10.1088/1742-6596/370/1/012020.
[22] T. Shinagawa, K. Shibata, O. Shimomura, M. Chigane, R. Nomura, M. Izaki, Solution-processed high-haze ZnO pyramidal textures directly grown on a TCO substrate and the light-trapping effect in Cu_2O solar cells, J. Mater. Chem. C 2 (2014) 2908.
[23] A. Taurino, M. Catalano, A. Cretì, M. Lomascolo, C. Martucci, F. Quaranta, Substrate-Au catalyst influence on the growth of ZnO nanorods, Mater.s Sci. Engng. B 172 (2010) 225–230.
[24] Y.H. Hu, Y.C. Chen, H.J. Xu, H. Gao, W.H. Jiang, F. Hu, Y.X. Wang, Texture ZnO thin-films and their application as front electrode in solar cells, Engineering 2 (2010) 973.
[25] T. Fu, Y.G. Shen, Surface growth and anomalous scaling of sputter-deposited Al films, Physica B 403 (2008) 2306–2311.
[26] Tun-Yuan Chiang, Ching-Liang Dai, Der-Ming Lian, Influence of growth temperature on the optical and structural properties of ultrathin ZnO films, J. Alloys Compd. 509 (2011) 5623–5626.